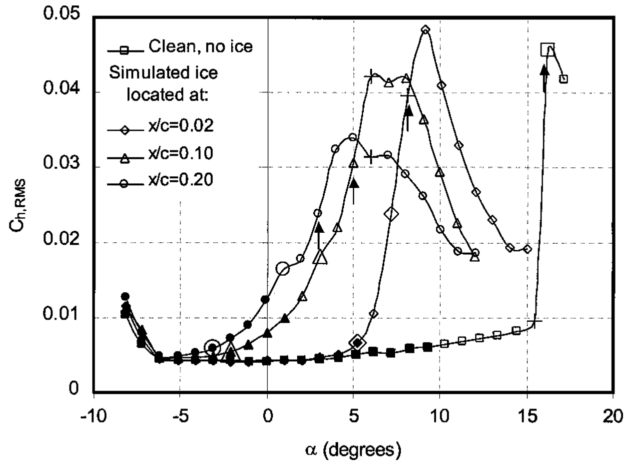

Fig. 3 Unsteady rms hinge-moment coefficient for the clean and simulated-iced airfoil at three ice-shape locations. Corresponding linear lift-curve regions for each case are denoted by ▲, ●, ■, whereas △, ○, □ represent the nonlinear regions. The outlined symbols of the simulated-iced cases denote the locations of the $C_{h,\mathrm{rms}}$ break. The enlarged symbols indicate the angle at which the C_h break occurred, and ↑ represent the angle at which the upper surface flowfield was completely separated. The + denote the location of maximum lift.

$C_{h,\mathrm{rms}}$ values were 30% greater than the clean airfoil values at corresponding angles of attack.

The $C_{h,\mathrm{rms}}$ breaks of the simulated-iced airfoil occurred in the linear lift-curve regions, apparent from the solid symbols in the figure. Evidence suggests that the increasing unsteadiness of the ice-induced separation bubble caused an increase in $C_{h,\mathrm{rms}}$ before the rapid bubble growth caused a nonlinearity in C_ℓ. The rise in the unsteady parameter served as a precursor to several subsequent flowfield events. In each simulated-iced case, as the angle of attack increased, the $C_{h,\mathrm{rms}}$ broke from the clean airfoil values and was followed by a break in C_h, complete upper surface flow separation, and finally $C_{\ell\,\max}$. Table 1 shows that the break in $C_{h,\mathrm{rms}}$ occurred approximately 2–4 deg before the C_h break and 3–9 deg before $C_{\ell\,\max}$ was reached.

Conclusions

The rms hinge-moment coefficient provides a clear distinction between clean and simulated-iced airfoils even before the nonlinear-lift range is reached. Simulated-iced $C_{h,\mathrm{rms}}$ values differ significantly from those of the clean case before the C_h break (when flow reattachment reaches the flap) and prior to flow separation over the entire airfoil surface.

If the pilot were to have access to unsteady hinge-moment data during flight, a notable departure from the expected clean values could provide warning of performance and control degradation. Rather than relying on the maximum control surface deflection or stall angle based on the clean airfoil case, the pilot could be alerted to possible flap and angle of attack restrictions derived from real-time performance monitoring based on this rms hinge-moment parameter.

Acknowledgments

This work was supported in part by a Critical Research Initiatives Grant from the University of Illinois at Urbana–Champaign. The authors would also like to thank the Federal Aviation Administration Technical Center for the use of the NACA 23012m airfoil model, and Andy Broeren and Sam Lee at Illinois for their assistance.

References

[1]Trunov, O. K., and Ingelman-Sundberg, M., "On the Problem of Horizontal Tail Stall Due to Ice," Swedish-Soviet Working Group on Scientific-Technical Cooperation in the Field of Flight Safety, The Swedish Board of Civil Aviation and USSR Ministry of Civil Aviation, Moscow, Rept. JR-3, Feb. 1985.

[2]Johnson, C. L., "Wing Loading, Icing and Associated Aspects of Modern Transport Design," *Journal of the Aeronautical Sciences*, Vol. 8, No. 2, 1940, pp. 43–54.

[3]Bradley, J. J., "A Safety and Economics Study of Aircraft Ice Protection," M.S. Thesis, Dept. of Aeronautical and Astronautical Engineering, Univ. of Illinois at Urbana–Champaign, IL, Aug. 1999.

[4]Bragg, M. B., "Aircraft Aerodynamic Effects due to Large Droplet Ice Accretions," AIAA Paper 96-0932, Jan. 1996.

[5]Lee, S., Dunn, T., Gurbacki, H. M., Bragg, M. B., and Loth, E., "An Experimental and Computational Investigation of Spanwise-Step-Ice Shapes on Airfoil Aerodynamics," AIAA Paper 98-0490, Jan. 1998.

[6]Lee, S., and Bragg, M. B., "Effects of Simulated-Spanwise Ice Shapes on Airfoils: Experimental Investigation," AIAA Paper 99-0092, Jan. 1999.

[7]Lee, S., and Bragg, M. B., "Experimental Investigation of Simulated Large-Droplet Ice Shapes on Airfoil Aerodynamics," *Journal of Aircraft*, Vol. 36, No. 5, 1999, pp. 844–850.

[8]Gurbacki, H. M., "Sensing Aircraft Icing Effects from Flap Hinge-Moment Measurement," M.S. Thesis, Dept. of Aeronautical and Astronautical Engineering, Univ. of Illinois at Urbana–Champaign, IL, May 2000.

[9]Barlow, J. B., Rae, W. H., and Pope, A., "Boundary Corrections I: Basics and Two-Dimensional Cases," *Low-Speed Wind Tunnel Testing*, 3rd ed., Wiley, New York, 1999, pp. 328–366.

Flow Quality Improvements in a Blowdown Wind Tunnel

H. Sundara Murthy,* R. S. Verma,*
S. P. Jagadeeswarachar,* and Rajan Kumar*
National Aerospace Laboratories,
Bangalore 560 017, India

Introduction

A HIGH level of flow unsteadiness in wind tunnels is undesirable because it can influence certain aerodynamic phenomena, such as the location of boundary-layer transition and subsequent growth of the turbulent boundary layer on models. It can also lead to problems in carrying out or can even impede certain dynamic measurements in the tunnel. Although flow unsteadiness is a generic term covering velocity fluctuations (turbulence), pressure fluctuations (acoustic noise), and temperature (entropy) fluctuations in freestream, acoustic noise is usually dominant in conventional subsonic/transonic tunnels and flow unsteadiness in wind tunnels is normally assessed by noise level measurements.

Noise levels in the National Aerospace Laboratories (NAL) 1.2-m blowdown wind tunnel were found to be high, which resulted in reduced accuracy of certain dynamic measurements and data interpretation problems. The principal sources of the noise were found to be the pressure regulating valve and the perforated wall test section in the tunnel (see Fig. 1a). To overcome these problems a major refurbishment program aimed at reducing the high noise levels in the tunnel was undertaken. The goal was to reduce the pressure fluctuation coefficient Cp_{rms} (equal to $\bar{P}/q$, where $\bar{P}$ is the rms static pressure fluctuation in the test section and q is the freestream dynamic pressure) to $\leq 1\%$ in the subsonic and transonic speed regime and $\leq 0.2\%$ at supersonic speeds. This Note presents brief details of the modifications incorporated and the results of wind-tunnel tests conducted to evaluate the flow quality improvements achieved.

Details of Modification

A relative assessment of different concepts tried elsewhere indicated that installation of acoustic baffles in the settling chamber

Received 19 October 2000; revision received 31 January 2001; accepted for publication 1 February 2001.

*Scientist, National Trisonic Aerodynamic Facilities.

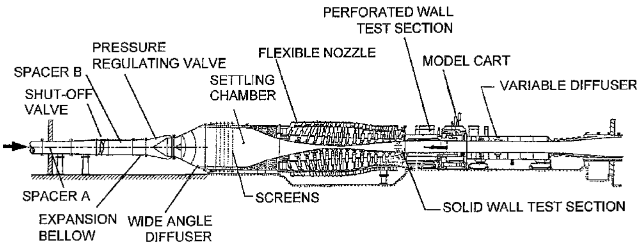

a) Original tunnel configuration

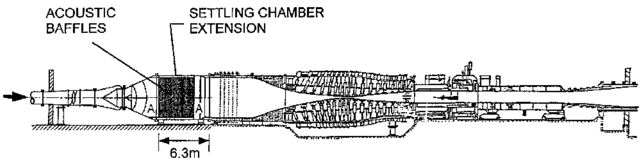

b) Modified tunnel configuration

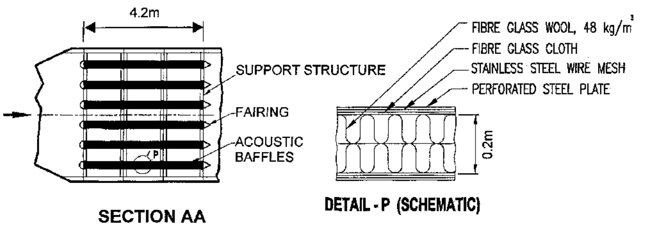

c) Details of acoustic baffles

Fig. 1 Original and modified layouts of the NAL 1.2-m tunnel.

would be the optimum solution to improve the flow quality in the NAL 1.2-m tunnel. Because the existing settling chamber did not have adequate space for installing the proposed acoustic baffles, some changes were made in the layout of the upstream region of the tunnel to facilitate installation of acoustic baffles (Fig. 1). Two spacer ducts (shown as spacers A and B in Fig. 1a) were removed from the tunnel circuit and the resulting space was utilized to extend the existing settling chamber by fixing a newly fabricated shell of 4.3 m diameter by 6.3 m length upstream of the existing settling chamber (Fig. 1b). Six acoustic baffles, each of 4.2 m length by 0.2 m thickness, were installed vertically in the shell. The baffles, designed using methods and data of Ref. 1, consist of fiber glass wool pads wrapped in fiberglass cloth and covered with two protective facings formed by a stainless steel wire mesh and an outer perforated steel plate (Fig. 1c). The estimated overall attenuation level provided by the baffles was about 15 dB, which was adequate to achieve the set goal at test section Mach number $M \geq 0.5$. However, the use of longer length baffles that could provide an attenuation of 25 dB needed to meet the goal at $M < 0.5$ was not possible due to space constraints. The baffles are mounted in a support structure featuring three separate support modules, each of 1.4-m length, for ease of assembly/disassembly. Semi-cylindrical and wedge-shaped fairings are provided, respectively, at the leading and trailing edges of each baffle to obtain a streamlined shape.

Wind-Tunnel Tests

Wind-tunnel tests were carried out at $M = 0.2$–2.5, and pressure fluctuation measurements were made in the settling chamber (using a total pressure probe), the solid-wall (SW) and perforated-wall (PW) test sections (using a 10-deg cone), and the plenum chamber (using a miniature pressure transducer) to assess the flow quality improvements. [The SW test section is employed for tests at supersonic and subsonic speeds, and the PW test section is inserted downstream of the SW test section for tests at transonic speeds (Fig. 1a). The PW test section is moved out of the tunnel circuit for supersonic/subsonic speed operation.] The pressure signals were processed to obtain constant bandwidth rms amplitude spectra and broadband rms levels in a frequency range of 0–10 kHz. These tests were conducted just before and immediately after incorporating the modifications to obtain comparative data.

Results and Discussions

Comparison of Pressure Fluctuations Before and After Modification

Pressure fluctuations data in the settling chamber and the two test sections obtained before and after modification are plotted against test-section Mach number in Figs. 2–4. The broadband level of total pressure fluctuations in the settling chamber, $\bar{P}_0$, is expressed as a percentage of mean total pressure P_0 and the broadband level of test-section static pressure fluctuations is presented in terms of Cp_{rms} (defined earlier). Installation of acoustic baffles resulted in substantial reductions in the broadband levels of pressure fluctuations in both the settling chamber and the SW test section (Figs. 2a and 2b). The overall attenuation in the settling chamber varied from 13 to 19 dB for test-section Mach numbers between 0.2 and 2.5 (Fig. 2a), which was close to the design estimate of 15 dB. The test-section noise reduction goal has been met at supersonic speeds and also at Mach numbers between 0.5 and 0.7, and accurate dynamic measurements (an example of which is presented later) are now possible at supersonic speeds in the SW test section. However, as predicted, the broadband levels at $M < 0.5$ did not meet the set goal.

Typical spectra showing nondimensional intensities, $\Delta P_0/P_0$ and $\Delta P/q$ (where ΔP_0 and ΔP are the rms intensities of total pressure fluctuations and static pressure fluctuations in a bandwidth Δf at frequency f, respectively) indicate that significant reductions in intensities have occurred at all frequencies beyond 100 Hz (Fig. 3). Although a few tones between 150 and 800 Hz that contributed

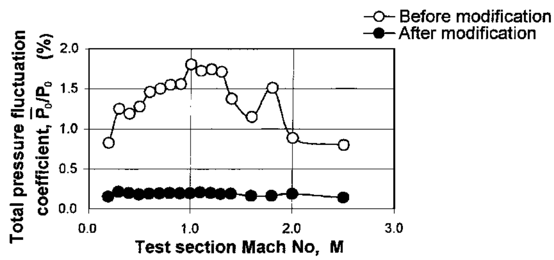

a) Settling chamber

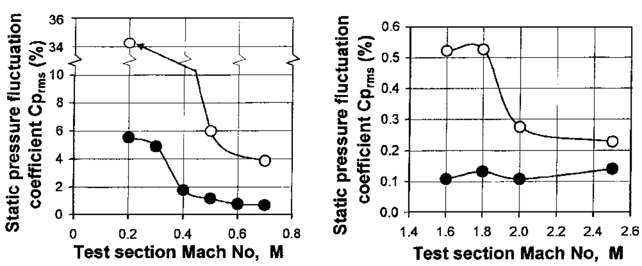

b) SW test section

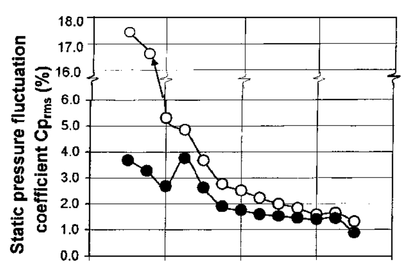

c) PW test section

Fig. 2 Comparison of broadband levels of total pressure fluctuations in settling chamber and static pressure fluctuations in SW and PW test sections, before and after tunnel modification.

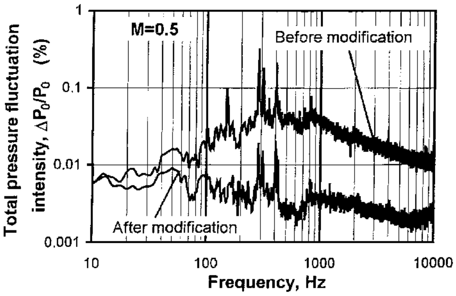

a) Settling chamber

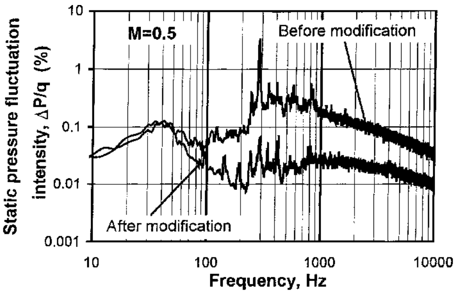

b) SW test section

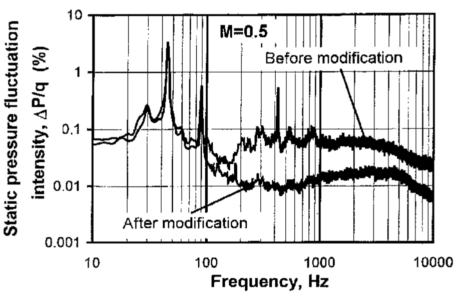

c) PW test section

Fig. 3 Comparison of spectra of pressure fluctuations in settling chamber and SW and PW test sections, before and after tunnel modification.

significantly to the broadband levels in the settling chamber and the SW test section of the original tunnel have not been completely suppressed, their amplitudes have substantially attenuated, resulting in corresponding reductions in their contributions to the broadband levels in the modified tunnel.

Large reductions occurred in the noise levels in the PW test section at Mach numbers up to 0.4, but the reduction was quite small at higher Mach numbers (Fig. 2c), primarily because the present modification (which was limited to the upstream region of the tunnel) did not attenuate a strong tone (and its harmonic) generated in the PW test section at a frequency between 45 and 65 Hz, which accounts for nearly 90% of the broadband level at $M = 0.5$–0.7 (Fig. 3c). Precise reasons for the generation of this tone, which was found in both the test section and the plenum chamber with approximately the same amplitude, are not clear. Although the overall noise reduction goal has not been met, attenuation of pressure fluctuation intensity at frequencies >100 Hz (see Fig. 3c) has improved the buffet onset measurement capability in the PW test section, as discussed later.

Flow Quality Comparisons with Other Tunnels

A widely accepted criterion for judging flow quality (with regard to flow unsteadiness) in wind tunnels is the broadband level of the test-section centerline static pressure fluctuations on a 10-deg cone. A comparison of these data from the present measurements in the original and modified NAL 1.2-m tunnel with data from some other well-known wind tunnels[2–9] is shown in Fig. 4. It is seen

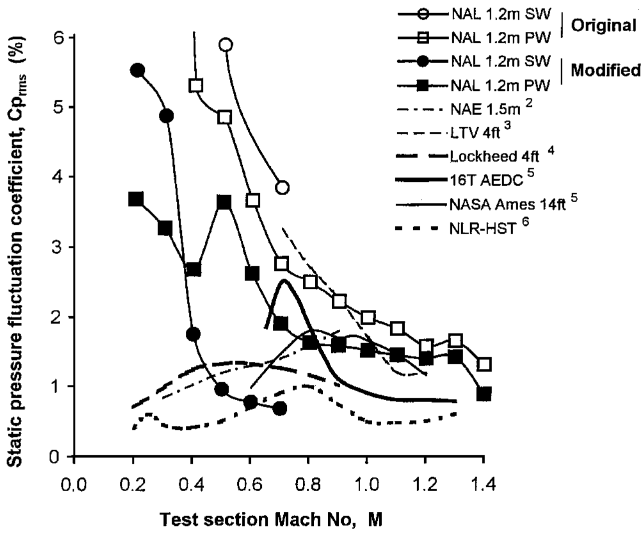

a) Subsonic/transonic speeds

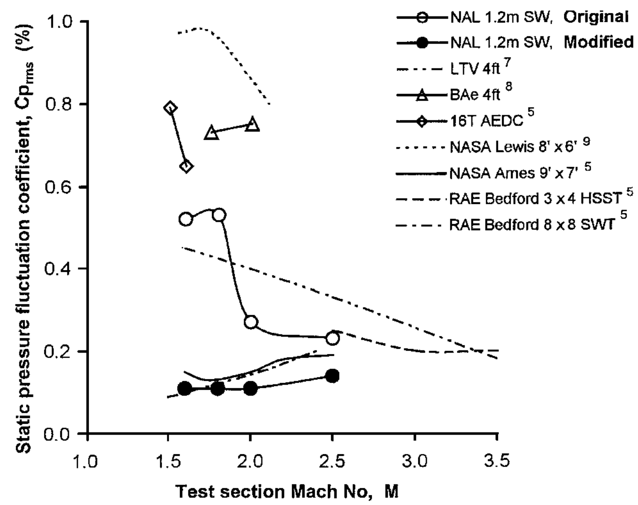

b) Supersonic speeds

Fig. 4 Test section centerline noise levels in the NAL 1.2-m tunnel compared with other tunnels.

that the noise levels at supersonic speeds and also at $M = 0.5$–0.7 in the SW test section of the NAL 1.2-m tunnel are among the lowest. However, the noise level in the PW test section is still relatively high, primarily because a strong, low-frequency tone generated in the PW test section has not been attenuated, as noted earlier.

Impact of Flow Quality Improvements

Two examples of beneficial effects of the reduction in test-section flow unsteadiness achieved by the present modification are noted hereafter.

The reduced level of test-section flow unsteadiness has considerably improved the suitability of the tunnel to make buffet onset measurements. Figure 5a shows a plot of the test-section flow unsteadiness parameter, $\sqrt{[nF(n)]}$ (equal to $\Delta P/q\ \sqrt{(\Delta f/f)}$ at selected frequencies covering the range of wing-bending natural frequencies f_{wb} of typical aircraft models in this tunnel against Mach number for the original and the modified tunnel. This parameter is assessed in relation to the well-known Mabey's criteria for light buffet onset measurements.[10] Because of the present modification, the flow unsteadiness parameter has improved from the marginal region in the original tunnel to adequate region in most cases. Consequently, the measurement of light buffet onset

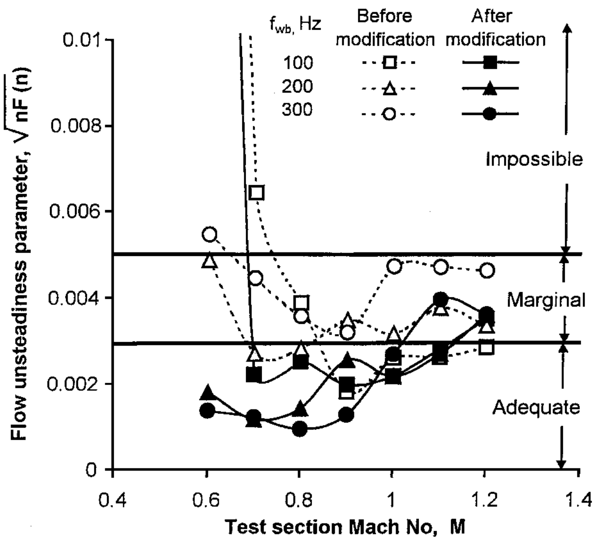

a) Criteria for light buffet onset measurements

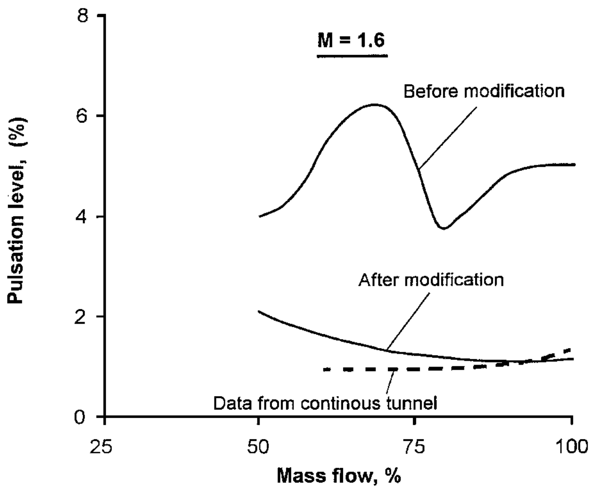

b) Comparison of pulsation measurements in air intake models

Fig. 5 Impact of improved flow quality on dynamic measurements in tunnel.

should yield more consistent and accurate data in the modified tunnel.

Figure 5(b) shows a comparison of pulsation level data (which are derived from unsteady total pressure distribution measurements across the engine face location) obtained on an aircraft intake model in the modified tunnel with data obtained on a similar model in the original tunnel, as well as a closed-circuit continuous tunnel. The pulsation levels measured in the original tunnel were 4–5 times higher than those measured in the continuous tunnel, primarily because the data were vitiated by the high levels of test-section flow unsteadiness, and the data were therefore considered erroneous. The pulsation levels measured in the modified tunnel, which are substantially lower and also close to those obtained in the continuous tunnel, are considered to reflect reality.

Conclusions

Acoustic baffles installed in the extended settling chamber of the NAL 1.2-m tunnel have substantially reduced the noise levels in its settling chamber and the SW test section. The quieter test-section flow has led to 1) a substantial improvement in the measurement accuracy of pulsation level data in air-intake models at supersonic speeds and 2) an improvement in light buffet onset measurement capability at subsonic/transonic speeds in the tunnel. However, the noise level in the PW test section is still high. Acoustic treatment of the plenum chamber aimed at mitigating the low-frequency tone observed in the PW test section is planned as a follow-on action.

References

[1]Doelling, N., "Dissipative Mufflers," *Noise Reduction*, edited by L. L. Beranek, McGraw–Hill, New York, 1960, pp. 434–451.

[2]Ohman, L. H., and Brown, D., "Performance of the New Roll-In Roll-Out Transonic Test Section of the NAE 1.5m × 1.5m Blowdown Wind Tunnel," *Proceedings of the 17th Congress of the International Council of the Aeronautical Sciences*, International Council of Aerospace Sciences and AIAA, Reston, VA, 1990, pp. 363–387.

[3]Cooksey, J. M., and Arnold, J. W., "Transonic Flow Quality Improvements in a Blowdown Wind Tunnel," *Journal of Aircraft*, Vol. 10, No. 9, 1973, pp. 554–560.

[4]Whitfield, E., "Noise and Flow Management in Blowdown Wind Tunnels," *Wind Tunnel Design and Testing Techniques*, CP174, AGARD , 1975, pp. 6-1–6-8.

[5]Dougherty, N. S., Jr., and Fisher, D. F., "Boundary-Layer Transition on a 10-Degree Cone: Wind-Tunnel/Flight-Data Correlation," AIAA Paper 800154, Jan. 1980.

[6]Ross, R., and Rohne, P. B., "Noise Environment in the NLR Transonic Wind Tunnel HST," National Aerospace Labs., Amsterdam, NLR TR 74128U, Aug. 1973.

[7]Ziegler, C. E., "Pressure Fluctuation at Supersonic Mach Numbers in the Loral Vought Systems High Speed Wind Tunnel," Loral Vought Systems, Dallas, Texas, Oct. 1984.

[8]Greening, E. S., "Modifications to the B.A.C. 4 ft H.S.T. Settling Chamber to Improve the Tunnel Flow Quality," British Aircraft Corporation, Preston, England, U.K., March 1973.

[9]Karabinus, R. J., and Sanders, B. W., "Measurements of Fluctuating Pressures in 8- by 6-Foot Supersonic Wind Tunnel for Mach Number Range of 0.56 to 2.07," NASA TM X - 2009, May 1970.

[10]Mabey, D. G., "Flow Unsteadiness and Model Vibration in Wind Tunnels at Subsonic and Transonic Speeds," Aeronautical Research Council, London, CP 1155, Oct. 1970.

Concise Orthogonal Representation of Supercritical Airfoils

G. M. Robinson*
Defence Evaluation and Research Agency, Farnborough, England GU14 6TD, United Kingdom
and
A. J. Keane†
University of Southampton, Southampton, England SO17 1BJ, United Kingdom

Introduction

THE combination of optimization algorithms and computational fluid dynamics offers promise for the development of improved aerodynamic designs. Optimization strategies have a common requirement for representation of geometry by a number of design parameters. For wing design the parameterization is generally separable into a representation of the planform and the representation of airfoil sections at a number of spanwise positions. The representation of airfoil sections is considered here with particular emphasis on the requirements of conceptual wing design.

The choice of representation depends on the type of optimization study. For two-dimensional airfoil design, representations are usually required that allow novel airfoil designs to be found. However,

Received 12 December 2000; revision received 28 January 2001; accepted for publication 7 February 2001.

*Research Fellow; currently Chief Aerodynamicist, Farnborough-Aircraft.com, Building P71, Farnborough, England, U.K.

†Professor of Computational Engineering, Director BAE Systems/Rolls-Royce University Technology Partnership for Design, School of Engineering Sciences, Highfield.